



# Bulletin of the Mineral Research and Exploration

<http://bulletin.mta.gov.tr>



## A graph method for interpretation of magnetic anomalies over 2D dikes and vertical faults

İbrahim KARA<sup>a</sup>, Oya TARHAN BAL<sup>a\*</sup> and Anisya B.TEKKELİ<sup>a</sup>

<sup>a</sup>*İstanbul University-Cerrahpaşa, Engineering Faculty, Department of Geophysical Engineering, İstanbul, Türkiye*

Research Article

### Keywords:

Magnetic Interpretation,  
2D Dike, Vertical Fault,  
Graph Method.

### ABSTRACT

Simple geometric assumptions for dikes and faults are often used for interpreting the parameters of these structures from magnetic anomalies. The magnetic anomaly of a 2D dike or a vertical fault consists of two components; one with even and the other with odd symmetries. The function resulting from the ratio of the even and odd components is independent from the amplitude coefficient. The abscissa of the half-maximum of the even component and the maximum of the odd component of a dike or a vertical fault is related to its depth and its half-width. Incorporating this relation into the corresponding equations for dikes and vertical faults, the half-width value can be eliminated from the equations. Thus, the resulting ratio can be used for determining the model parameters. Using the ratio of the even component to the odd component for given distances, curves can be obtained for different depth-index parameter pairs, and from the graph of these curves, parameters of 2D dikes and vertical faults can be determined. The validity of the method is tested using synthetic models for dike and vertical fault cases. The method is also implemented on two different field data, and the results obtained are compared to previous studies.

Received Date: 02.01.2021  
Accepted Date: 16.04.2021

## 1. Introduction

Dike and vertical fault models are used often in magnetic interpretation. Many researchers have interpreted the anomalies of these structures by decomposing the anomalies into their origin-symmetric even and odd components. Hutchison (1958) uses a logarithmic curve fitting method, Bhimasankaram et al. (1978) use Fourier transforms, in Kara et al. (1996) and Kara (1997) a method using correlation factors and integration nomograms is presented, in Rao et al. (1973) two methods are presented using the horizontal derivative of the anomaly, and in Atchuta Rao and Ram Babu (1981) a method using nomograms is presented.

Even though, nowadays 2D and 3D inversions are widely used for recovering subsurface structures, they often result within misleading results due to non-uniqueness of the solutions. For these reasons, calculations by assuming simple source geometries are still implemented for recovering model parameters for such structures. Some recent examples of methods developed to interpret anomalies of dikes and other simple geometries can be given as follows; Abdelrahman and Essa (2015) employed second derivative anomalies to obtain depth and shape properties of simple geological models, Abo-Ezz and Essa (2016) used linearized magnetic anomaly formula for simple geometries applied least-squares method. Essa and Elhussein (2017) recovered model

Citation Info: Kara, İ., Tarhan Bal, O., Tekkeli, B. A. 2022. A graph method for interpretation of magnetic anomalies over 2D dikes and vertical faults. Bulletin of the Mineral Research and Exploration 168, 1-10. <https://doi.org/10.19111/bulletinofmre.928467>

\*Corresponding author: Oya TARHAN BAL, [tarhan@istanbul.edu.tr](mailto:tarhan@istanbul.edu.tr)

parameters of a dipping dike using second horizontal gradient anomalies.

In this study, a method is proposed to recover model parameters of dipping dikes and vertical faults from magnetic field anomalies. For such simple structures assumptions, implementing least-squares inversion or global optimization methods do not provide much advantage since the calculations are fast. Hence, applying a graph method is preferred due to its simplicity in code development and implementation.

In the method, depth and index parameters are delineated from the intersection point of a set of curves, which are obtained from the ratio of the even component to the odd component. Half-width of the structure is determined from its relation to the half-maximum of the even component and the abscissa of the maximum of the odd component. The method presented in this study is tested on synthetic models for both dike and vertical fault cases, and then, implemented on field data.

## 2. Method

In the method presented in this study, developed in order to interpret magnetic anomalies due to dikes and vertical faults, following notations and assumptions are made.

On a Cartesian coordinate system, the axis Y is assumed to be aligned with the strike direction of the 2D anomalous structure and the X axis showing the direction of the measurement profile (Figure 1a, b and c).  $i$  is the geomagnetic inclination in the survey area, the azimuth of the profile according to the magnetic north is denoted with  $\alpha$ , dipping angle of the dike or fault is shown with  $d$ ,  $k$  is the susceptibility contrast,  $T$  is the nominal value of the total field intensity,  $R=\sin\theta$  for dikes, and  $R=\cos\theta$  for vertical faults.

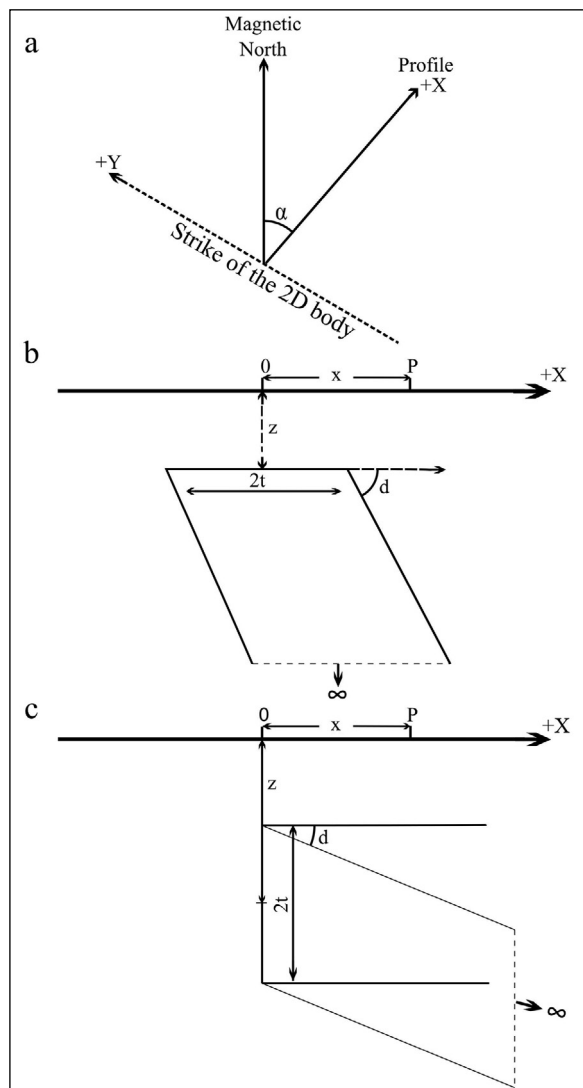


Figure 1- Generalized presentation of 2D dikes and vertical faults; a) view from top, showing magnetic north, the profile and the strike of the 2D body, b) cross-section of a dike and c) cross-section of a vertical fault.

According to the notations defined above, variation of the amplitude coefficient and the index parameter may be given as in Table 1 for total, vertical, and horizontal magnetic anomaly components respectively. In the table,  $I=\tan^{-1}(\tan(i)/\cos(\alpha))$ .

Table 1- Amplitude coefficient and index parameters for different magnetic field components.

| Anomaly in       | Amplitude Coefficient (M)                        | Index Parameter ( $\theta$ ) |
|------------------|--|------------------------------|
| Total field      | $2kTS(1-\cos^2i-\sin^2\alpha)$                   | $2I-d-90^\circ$              |
| Vertical field   | $2kTS(1-\cos^2i \sin^2\alpha)^{1/2}$             | $I-d$                        |
| Horizontal field | $2kTS \sin\alpha (1-\cos^2i \sin^2\alpha)^{1/2}$ | $I-d-90^\circ$               |

## 2.1. Implementation of the Method for Dipping Dikes

The magnetic anomaly ( $\Delta F$ ) due to a dipping dike (Figure 1b) at any point P(x) is given as below,

$$\Delta F = M \left\{ \cos\theta \left[ \tan^{-1} \left( \frac{x+t}{z} \right) - \tan^{-1} \left( \frac{x-t}{z} \right) \right] + \frac{1}{2} \sin\theta \ln \left[ \frac{(x+t)^2 + z^2}{(x-t)^2 + z^2} \right] \right\} \quad (1)$$

(Parker, 1963). In the equation, x is the distance of the observation point to the origin, z is the depth to the top of the dike, and t is the half-width. The Equation 1 may be expressed as the sum of the even (E) and the odd (F) components and given below,

$$\Delta F(x) = E(x) + F(x) \quad (2)$$

where,

$$E(x) = M \cos\theta \left[ \tan^{-1} \left( \frac{x+t}{z} \right) - \tan^{-1} \left( \frac{x-t}{z} \right) \right] \text{ (even)} \quad (3a)$$

$$F(x) = \frac{1}{2} M \sin\theta \ln \left[ \frac{(x+t)^2 + z^2}{(x-t)^2 + z^2} \right] \text{ (odd)} \quad (3b)$$

If we denote the abscissa corresponding to the half-maximum of E(x) and to the maximum of F(x) with s, the relation between them is given as:  $s = (z^2 + t^2)^{1/2}$  and solving this equation for t yields to

$$t = (s^2 - h^2)^{1/2} \quad (4)$$

If the value of the even component at any distance x is divided to the odd component for the same distance x, and denote the left-hand side using  $C_1$  and right-hand side with  $C_2$ , following expressions can be written,

$$C_1 = \frac{E(x)}{F(x)} \quad (5a)$$

$$C_2 = \frac{\cos\theta \left[ \tan^{-1} \left( \frac{x+t}{z} \right) - \tan^{-1} \left( \frac{x-t}{z} \right) \right]}{0.5 \sin\theta \ln \left[ \frac{(x+t)^2 + z^2}{(x-t)^2 + z^2} \right]} \quad (5b)$$

Since, t may be given as product of z and s, if the value of z is obtained, the value of t can be calculated using the Equation 4.

In the presented method, using Equation 5a,  $C_1$  is calculated from the values of the even and the odd components obtained from the observed field anomaly and the  $C_2$  is obtained by varying theoretical

$[\theta, z]$  pairs. One should notice that the  $C_1/C_2$  ratio is independent of the amplitude coefficient.

Each set of  $C_2$  values are calculated using Equation 5b for a value of z by varying  $\theta$  between  $0^\circ$ - $90^\circ$ ,  $90^\circ$ - $180^\circ$ ,  $180^\circ$ - $270^\circ$  or  $270^\circ$ - $360^\circ$  according to the Table 2. This process must be repeated by varying z to scan through all possible values. For each z, the value of  $\theta$  minimizing the difference between the observed and theoretical ratios,  $C_1$  and  $C_2$ , is determined and these z- $\theta$  pairs are plotted on a graph (z values against  $\theta$ ) as a curve. It's clear that the  $C_1$ - $C_2$  difference should be minimized for all distance values for the true values of the model parameters,  $\theta$  and z. Thus, when the curves for different distances are plotted together, the intersection point of these curves yields to the actual values of z and  $\theta$ . Once value of z is clear, t can be calculated using Equation 4. The flowchart of the process is given in Figure 2.

Table 2- Variation of  $\theta$  according to the extremum of the anomaly.

| Extremum                       | $\theta$        |  |
|--------------------------------|-----------------|--|
| Major positive anomaly towards | positive x axis | $0^\circ \leq \theta \leq 90^\circ$    |
| Major negative anomaly towards | negative x axis | $90^\circ \leq \theta \leq 180^\circ$  |
| Major negative anomaly towards | positive x axis | $180^\circ \leq \theta \leq 270^\circ$ |
| Major positive anomaly towards | negative x axis | $270^\circ \leq \theta \leq 360^\circ$ |

## 2.2. Implementation of the Method for Vertical Faults

Similar to the case in dikes, the magnetic anomaly ( $\Delta F$ ) at any point P(x) on the profile due to a vertical fault may be given as,

$$\Delta F = M \left\{ \cos\theta \ln \ln \left[ \frac{x^2 + (z+t)^2}{x^2 + (z-t)^2} \right]^{1/2} + \sin\theta \left[ \tan^{-1} \frac{x}{z+t} - \tan^{-1} \frac{x}{z-t} \right] \right\} \quad (6)$$

(Atchuta Rao and Ram Babu, 1981). Where, x is the distance of the observation point to the origin, z is the depth from surface to the half-thickness of the fault and t is the half-width of the fault. The Equation 6 may also be expressed using even (E) and odd (F) components,

$$\Delta F(x) = E(x) + F(x) \quad (7)$$

where,

$$E(x) = M \cos\theta \ln \left[ \frac{x^2 + (z+t)^2}{x^2 + (z-t)^2} \right]^{1/2} \quad (8a)$$

$$F(x) = M \sin\theta \left[ \tan^{-1} \frac{x}{z-t} - \tan^{-1} \frac{x}{z+t} \right] \quad (8b)$$

If the abscissa of the half-maximum of the  $E(x)$  and the maximum of  $F(x)$  is denoted with  $s$ , it's known that  $s=(z^2-t^2)^{1/2}$  and hence,

$$t=(z^2-s^2)^{1/2} \quad (9)$$

If the value of the even component at any distance  $x$  is divided to the odd component for the same distance  $x$ , following expressions can be written, where the left-hand side of the division is denoted using  $C_1$  and right-hand side with  $C_2$ ,

$$C_1 = \frac{E(x)}{F(x)} \quad (10a)$$

$$C_2 = \frac{\cos\theta \ln \left[ \frac{x^2 + (z+t)^2}{x^2 + (z-t)^2} \right]^{1/2}}{\sin\theta \left[ \tan^{-1} \frac{x}{z-t} - \tan^{-1} \frac{x}{z+t} \right]} \quad (10b)$$

Since the value of the  $t$  may be given in terms of  $z$  and  $s$ , the unknowns remaining in the Equation 10b are  $\theta$  and  $z$ . Once the value of  $z$  is obtained,  $t$  can be calculated using Equation 9. To obtain  $\theta$  and  $z$  for vertical faults, the same process given for the dike is applied (Figure 2).

### 3. Findings

#### 3.1. Theoretical Implementation on a Dike Anomaly

In this synthetic test, the following model parameters are employed;  $z=8$  m,  $t=4$  m, and  $\theta=50^\circ$ . The anomaly, obtained from the given model parameters, is shown in Figure 3a, and its even and odd components are shown in Figure 3b.

The proposed method is implemented using the values of the even and odd components between  $x=[1, 12]$  m. The set of curves obtained for these values are presented in Figure 4. The intersection point of these curves yields to the actual depth ( $z$ ) and index parameter ( $\theta$ ) values.

From the Figure 4, it's easy to note that the value of  $z=8$  m and  $\theta=50^\circ$ . The value of  $s=8.95$  m is also obtained from the Figure 3b. Using the obtained  $z$  and  $s$  values in Equation 4, the half-width value is obtained as  $t=4$  m. These values are the same of the actual

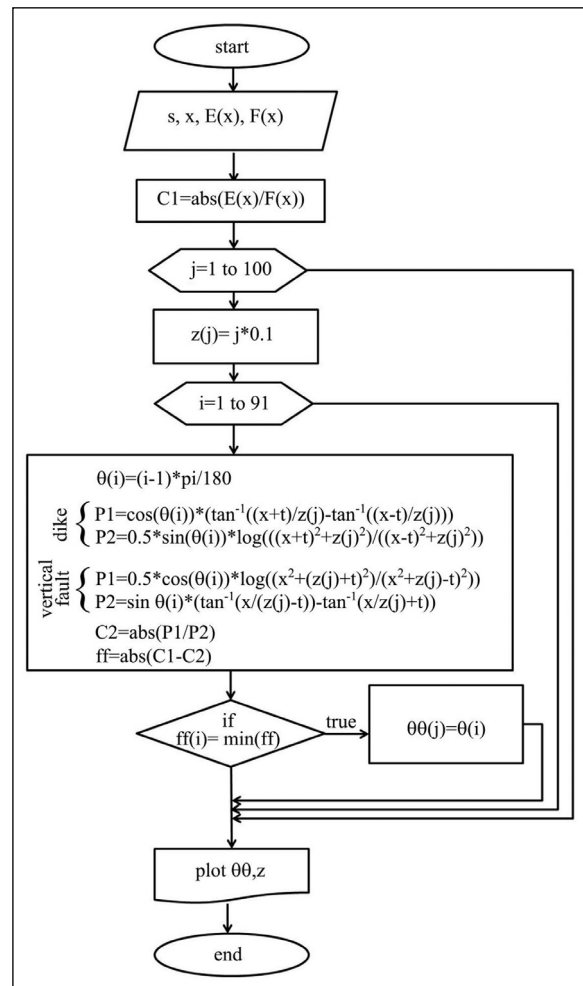


Figure 2- Flowchart to obtain a single curve.

values, justifying the proposed method to recover the model parameters.

In order to demonstrate the applicability of the method for noisy datasets, 5% Gaussian noise is applied on the data and the results of the algorithm are compared. 1000 realizations are performed for the described experiment. For the automated selection of  $\theta$  and  $z$  values, outliers are eliminated using 70% trimmed mean and thereafter the best intersection point is determined.

A sample noisy data and its even and odd components for  $x>0$  are shown in Figure 5; the set of curves obtained for the given noisy data is shown in Figure 6a. Each  $[\theta, z]$  pair, which are recovered from the 1000 realizations of the experiment, are shown in Figure 6b as a scatterplot; the value recovered for the sample noisy data is also marked in the figure. For the

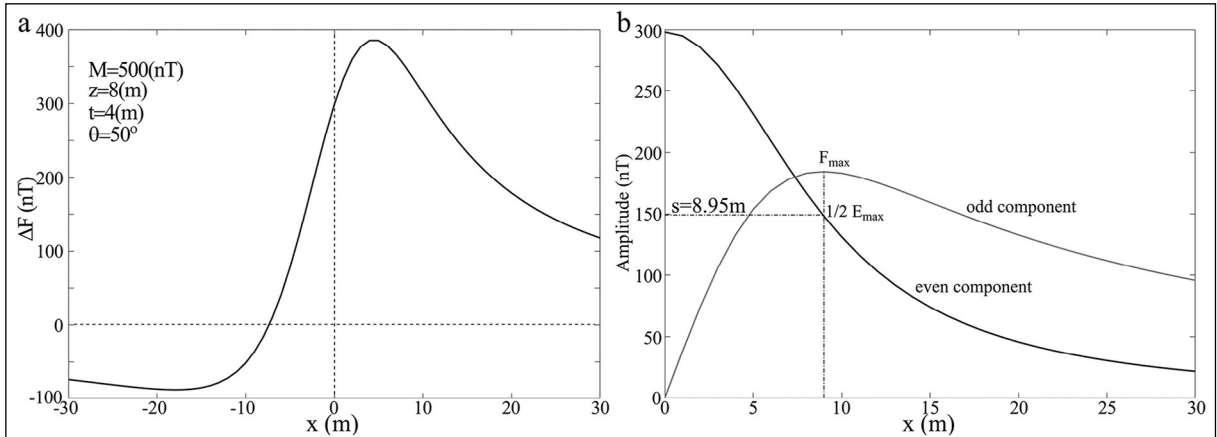


Figure 3- a) Calculated magnetic anomaly of the theoretical dike model and b) calculated even and odd components of the magnetic anomaly of the theoretical dike model.

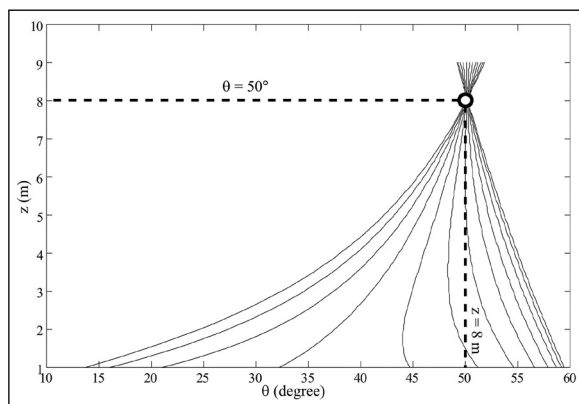


Figure 4- The set of curves obtained by the implementation of the method on the even and odd components due to the theoretical model.

introduced noise level, the experiment shows that the  $\theta$  values are scattered between [49, 51] degrees, and  $z$  values are varying between [7, 9] m. The experiment shows that the method can also be applied successfully to noisy datasets.

### 3.2. Implementation on Field Data of a Dike

For the implementation on field data, the data collected on a diabase dike located in Durham Triassic Basin in North Carolina, USA, previously interpreted by Won (1981) is sampled (Figure 7a, solid line). Thereafter the presented method is implemented by the decomposition of the data into its even and odd components (Figure 7b).

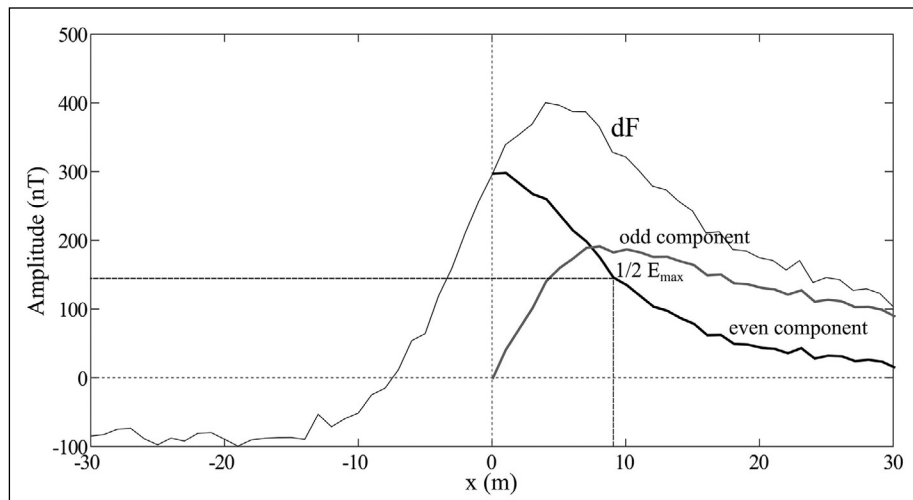


Figure 5- Magnetic anomaly of a theoretical dike model with 5% Gaussian noise ( $dF$ ), and its even and odd components for  $x>0$ .

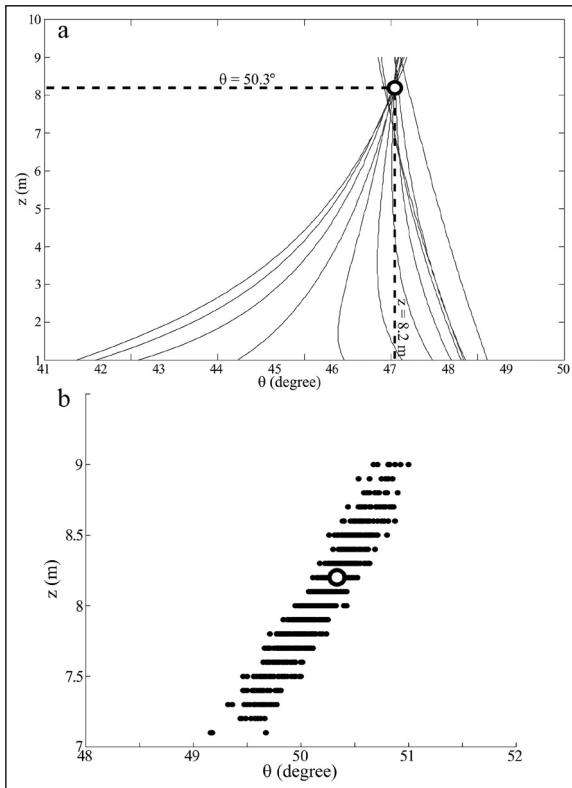


Figure 6- a) The set of curves obtained from the implementation of the method on data with 5% Gaussian noise and b) distribution of the  $[\theta, z]$  pairs obtained by the application of the method on noisy anomaly [for 1000 realizations]. The  $[\theta, z]$  pair obtained for the sample noisy data is shown with circle.

In the Figure 7b, the abscissa of the half-maximum of the even component yields to  $s=21.34\text{m}$ . When the proposed method is applied using the even and odd component values at  $x=10, 20, 30$ , and  $40\text{m}$  the curves

given in Figure 8 are obtained. From their intersection point  $z=8.4\text{m}$  and  $\theta=329^\circ$  values are determined. Using these values,  $t=19.62\text{m}$  is calculated using Equation 4.

At this stage, all the parameters except the amplitude coefficient ( $M$ ) are obtained. The value of  $M=346.1$  can be computed using Equation 3a and the

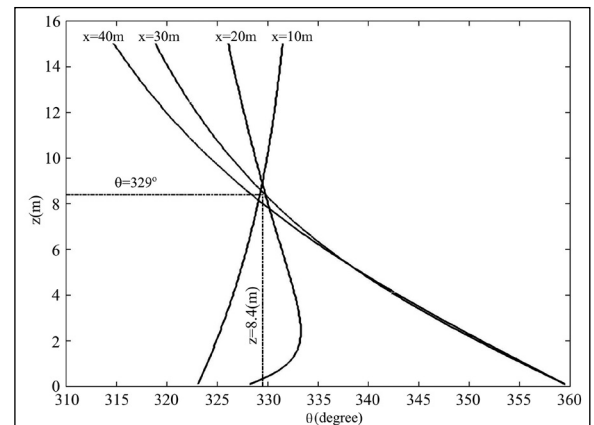


Figure 8- The set of curves obtained by the implementation of the proposed method using the even and odd components of the field anomaly.

synthetic anomaly can be plotted as seen in Figure 7a (dots) by using the recovered parameters. As seen in Figure 7a, the calculated and the observed anomalies are noticeably similar. These values are also similar to the results ( $z=7.97\text{ m}$ ,  $t=19.7\text{ m}$ ,  $\theta=292.6^\circ$ ) given by Won (1981).

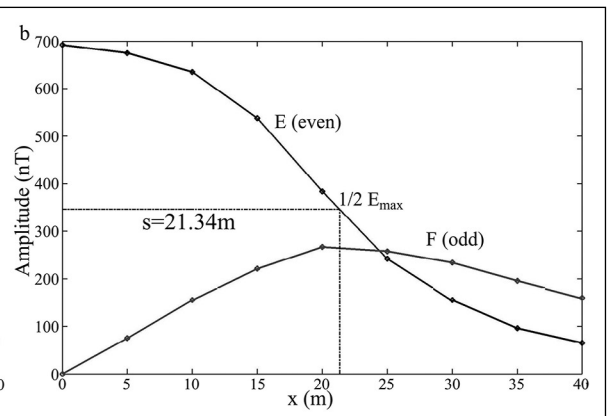
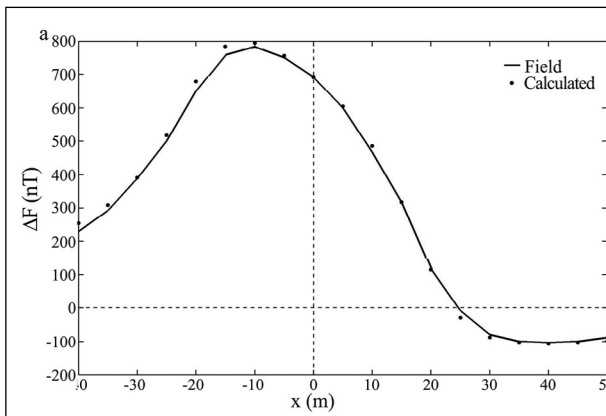


Figure 7- a) The vertical magnetic field anomaly (solid line) over a diabase dyke (Won, 1981), and the anomaly obtained from the model parameters recovered using the proposed method (dots) and b) even and odd component anomalies of the field data.

### 3.3. Theoretical Implementation on a Vertical Fault Anomaly

For this example, the anomaly for a vertical fault is calculated using following model parameters;  $M=500$  nT,  $z=10$  m,  $t=6$  m, and  $\theta=45^\circ$  and shown in Figure 9a. The even and the odd components calculated for this model are presented in Figure 9b.

The set of curves given in Figure 10 are obtained by the implementation of the proposed method employing the even and odd component anomalies for  $x=[1, 12]$  m interval. The intersection point of these curves should yield to the depth ( $z$ ) and index parameters ( $\theta$ ).

From the Figure 10, the intersection point of the curves yields to  $z=10$  m and  $\theta=45^\circ$ , and  $s=8$  m is obtained from Figure 9b. Incorporating these values in Equation 9, the half-width is calculated as  $t=6$  m. The values recovered by the proposed method are the same of the defined model parameters.

In order to show that the method is also valid for noisy data vertical faults, the results of the algorithm are tested after adding 5% Gaussian noise to the data due to the theoretical vertical fault. For the vertical fault case, the experiment is also performed with 1000 realizations. In the Figure 11, a sample noisy data and its even and odd components for  $x>0$  are shown; the set of curves obtained for the given data is given in Figure 12a. The  $[\theta, z]$  pairs obtained after performing 1000 realizations are presented as a scatterplot in the Figure 12b; the value obtained for the sample noisy

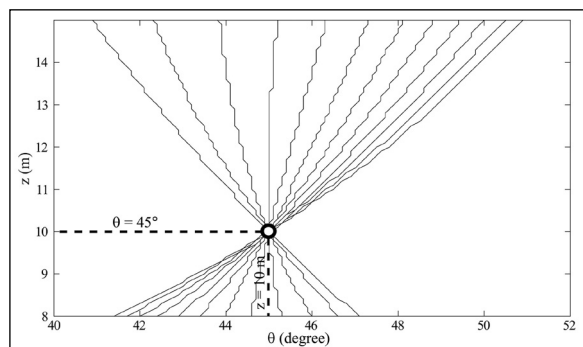


Figure 10- The set of curves, obtained by the implementation of the proposed method on the theoretical even and odd component anomalies due to the vertical fault.

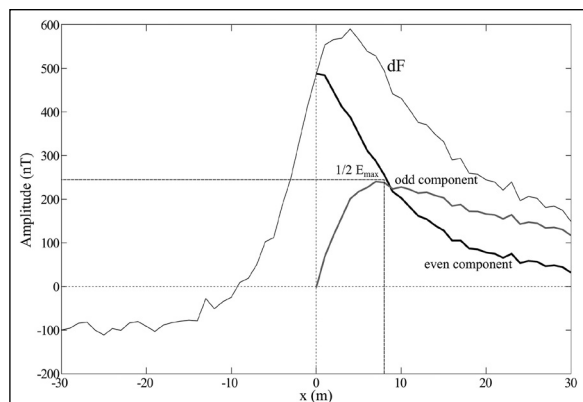


Figure 11- Magnetic anomaly of a theoretical fault model with 5% Gaussian noise ( $dF$ ), and its even and odd components for  $x>0$ .

data is also marked on the plot. For the introduced noise level, the experiment shows that the  $\theta$  values are scattered between [43.75, 46] degrees, and  $z$  values

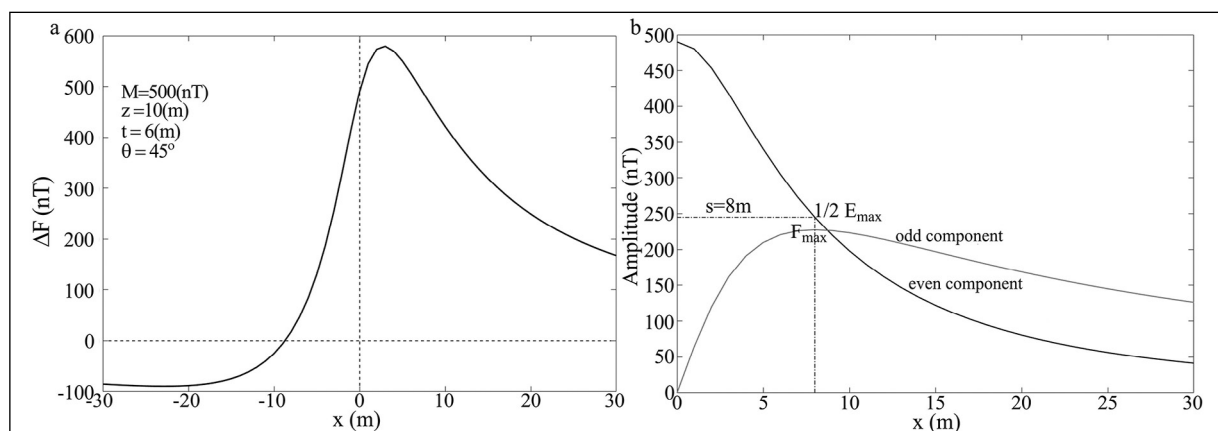


Figure 9- a) Calculated magnetic anomaly due to the theoretical vertical fault and b) even and odd components calculated using the theoretical vertical fault anomaly.

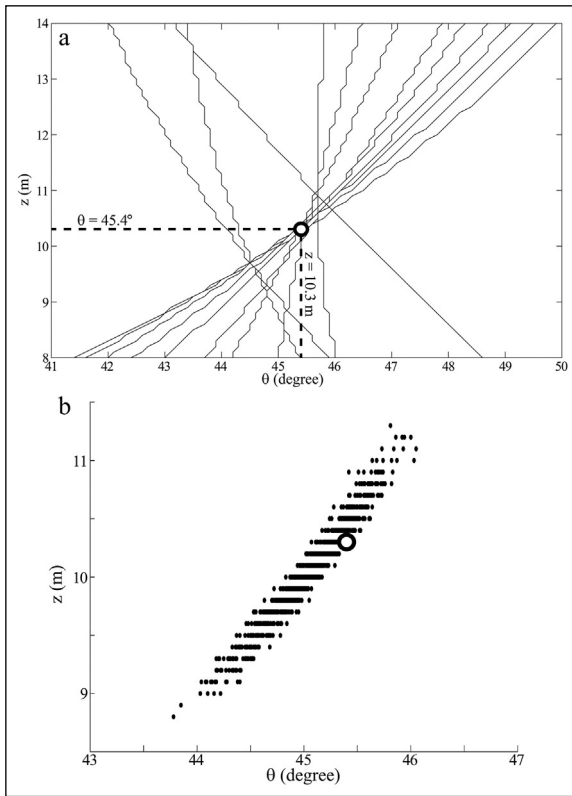


Figure 12- a) The set of curves obtained from the implementation of the method on data with 5% Gaussian noise and b) distribution of the  $[\theta, z]$  pairs obtained by the application of the method on noisy anomaly [for 1000 realizations]. The  $[\theta, z]$  pair obtained for the sample noisy data is shown with circle.

vary [8.7, 11.3] m. The experiment shows that the method can also be applied successfully on noisy datasets of vertical faults.

### 3.4. Implementation on Field Data of a Vertical Fault

For the implementation on the field data, the total magnetic field anomaly collected over the western margin of Perth Basin (Atchuta Rao and Ram Babu, 1981) is sampled with 2 km intervals (Figure 13, solid line) and the sampled anomaly is decomposed into its even and odd components (Figure 13b).

By the decomposition of this anomaly into its even and odd components,  $s=10.3$  km is delineated from the abscissa of the half-maximum of the even component and the maximum of the odd component (Figure 13b). When the proposed method is applied using the even and the odd components at  $x=2, 4, 6$ , and  $8$  km the set of curves given in Figure 14 are obtained. From the intersection point  $z=11$  km and  $\theta=33^\circ$  values are recovered, and using Equation 9  $t=4.12$  is calculated. The anomaly calculated using the recovered parameters is given in Figure 13a with dots.

In the Figure 13a, the agreement between the observed and the calculated anomalies is good, and the recovered model parameters are similar to the values estimated in the previous studies of Qureshi and Nalaye (1978), Atchuta Rao and Ram Babu (1981).

## 4. Discussion

Although multi-dimensional inversion methods, based on geometric discretion of the subsurface, are widely implemented using modern software and

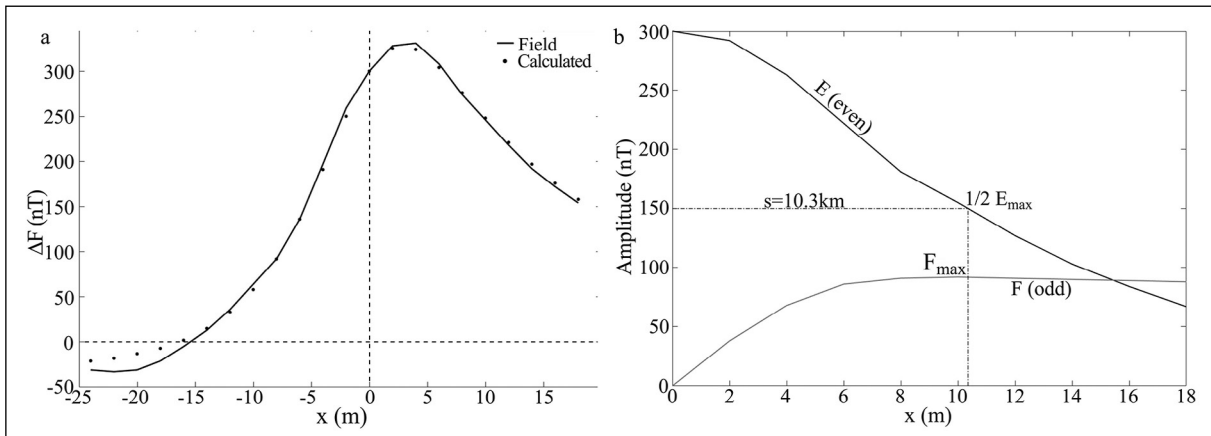


Figure 13- a) The total magnetic field anomaly over the western margin of Perth Basin (Atchuta Rao and Ram Babu, 1981; solid line) and the anomaly calculated using the model parameters recovered by the implementation of the proposed method (dots) and b) the even and odd component of the field anomaly for the vertical fault.

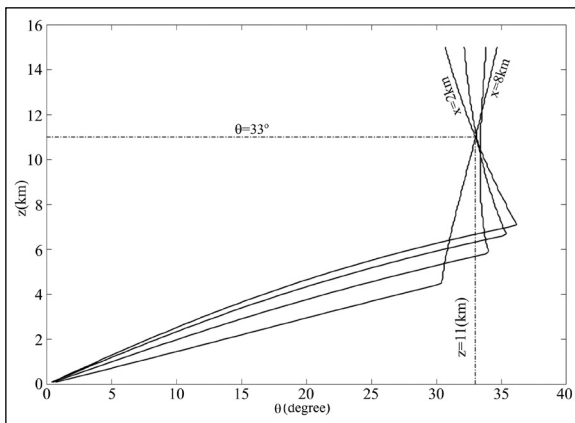


Figure 14- The set of curves obtained by the implementation of the proposed method.

methods, recovering dips and depths of structures correctly is rather difficult due to the lack of inherent depth resolution of the magnetic field data. Thus, graph and inversion methods, using simple structure geometries, are still implemented in recovering the parameters of the assumed structures.

The method implemented in this study, uses a graph based approach to recover model parameters from even and odd components of the measured data. Even though, the same approach can also be implemented using least-squares inversion, employing search via graphs method is equally effective since the calculations are fast and the non-uniqueness is rather low due to the assumed geometries.

The method estimates, depth, half-width and index parameters of dikes and vertical faults. The method is applied using even and odd components of the observed magnetic field anomaly. The method uses the ratio of the even component to the odd component for any distance  $x$ ; this ratio becomes independent of

the amplitude coefficient. The aim of the algorithm is to minimize the difference between the values obtained at several  $x$  distances for the observed data and the theoretical values calculated for different  $[θ, z]$  pairs. Since the true parameters are expected to minimize this difference for all distance values, parameters can be determined from the intersection of the curves obtained for different  $x$  distances. Then, half-width value ( $t$ ) is calculated using Equation 4. The proposed graph method is found to be effective on both dipping dike and vertical fault models for the calculated synthetic datasets.

The implementation of the presented interpretation method on field data for vertical fault anomalies proved to be successful in recovering the model parameters very similar to the previous interpretations of the same data by Qureshi and Nalaye (1978), Atchuta Rao and Ram Babu (1981). For the vertical fault data, the recovered parameters are compared to the mentioned previous studies in Table 3.

When the parameters recovered for the dike anomaly, provided in Won (1981), are compared, all parameters except the dip angle are found to be very close. However, the similarity of the observed and the calculated anomalies (Figure 7), suggests that the discrepancy in the recovered dip angle is in acceptable limits.

## 5. Results

In this study, a graph method to recover parameters from magnetic field anomalies due to dipping dikes and vertical faults is presented. The noise-free and noisy theoretical data examples have shown that the proposed method can determine the related model parameters, justifying the method.

Table 3- The recovered model parameters of the vertical fault, recovered by the method proposed in this study, and the results of the previous studies.

| Parameter                 | Qureshi and Nalaye (1978) | Achuta Rao and Ram Babu (1981) | Present Method |
|---------------------------|---------------------------|--------------------------------|----------------|
| Depth (z) to top in km    | 6.85                      | 7.2                            | 6.88           |
| Depth (z) to top in km    | 6.30                      | 7.9                            |                |
| Depth (H) to bottom in km | 11.55                     | 14.4                           | 15.12          |
| Depth (H) to bottom in km | 16.50                     | 15.7                           |                |
| θ in degrees              | -330                      | -315                           | -327 (33)      |

Since the true parameters are unknown, the field data examples are selected from previously interpreted data. Accordingly, data due to a diabase dike located in Durham Triassic Basin in North Carolina, USA, given in Won (1981), and data from a vertical fault in the western margin of Perth Basin, given in Atchuta Rao and Ram Babu (1981) are investigated, respectively.

The results have shown that the graph method described in this study is able to recover model parameters with values close to that of the previous studies. The only exception is determined for the dip angle of the diabase dike, the result of which was calculated to carry a  $36.4^\circ$  difference from the results given in Won (1981). However, the similarity between the observed and the calculated data shows that the given difference is within acceptable limits. The other parameters of the dike are obtained with values, which are very similar to that of Won (1981). For the data, collected over vertical fault, a more detailed comparison is realized since this data is interpreted in numerous studies. The comparison of results has shown that the method is able to recover all parameters of the given vertical fault successfully.

Considering synthetic and field data examples, the proposed graph method is found to be successful for recovering model parameters of dipping dikes and vertical faults from their magnetic anomalies.

### Acknowledgements

This paper is dedicated by his co-authors to the memory of Prof. Dr. İbrahim KARA. From the moment we stepped into the university, he guided and treated us as his own children, and inspired us as educators and researchers.

### References

- Abdelrahman, E. M., Essa, K. S. 2015. A new method for depth and shape determinations from magnetic data. *Pure and Applied Geophysics* 172(2), 439-460.
- Abo-Ezz, E. R., Essa, K. S. 2016. A least-squares minimization approach for model parameters estimate by using a new magnetic anomaly formula. *Pure and Applied Geophysics* 173(4), 1265-1278.
- Atchuta Rao, D., Ram Babu, H. V. 1981. Nomograms for rapid evaluation of magnetic anomalies over long tabular bodies. *Pure and Applied Geophysics* 119(5), 1037-1050.
- Bhimasankaram, V. L. S., Mohan, N. L., Seshagiri Rao, S. V. 1978. Interpretation of magnetic anomalies of dikes using Fourier transforms. *Geoexploration* 16(4), 259-266.
- Essa, K. S., Elhussein, M. 2017. A new approach for the interpretation of magnetic data by a 2-D dipping dike. *Journal of Applied Geophysics* 136, 431-433.
- Hutchison, R. D. 1958. Magnetic analysis by logarithmic curves. *Geophysics* 23(4), 749-769.
- Kara, İ. 1997. Magnetic interpretation of two-dimensional dikes using integration-nomograms. *Journal of Applied Geophysics* 36(4), 175-180.
- Kara, İ., Özdemir, M., Yüksel, F. A. 1996. Interpretation of magnetic anomalies of dikes using correlation factors. *Pure and Applied Geophysics* 147(4), 777-788.
- Parker Gay, S. 1963. Standard curves for interpretation of magnetic anomalies over long tabular bodies. *Geophysics* 28(2), 161-200.
- Qureshi, I. R., Nalaye, A. M. 1978. A method for the direct interpretation of magnetic anomalies caused by two-dimensional vertical faults. *Geophysics* 43, 179-188.
- Rao, B. S. R., Murthy, I. V. R., Visweswara Rao, C. 1973. Two methods for computer interpretation of magnetic anomalies of dikes. *Geophysics* 38(4), 710-718.
- Won, I. J. 1981. Application of Gauss's method to magnetic anomalies of dipping dikes. *Geophysics* 46(2), 211-215.